International Journal for Parasitology 49 (2019) 523–530

Contents lists available at ScienceDirect

International Journal for Parasitology

journal homepage: www.elsevier.com/locate/ijpara

Phylogeny of Myxobolidae (Myxozoa) and the evolution of myxospore appendages in the *Myxobolus* clade

Yang Liu [a,b], Alena Lövy [c], Zemao Gu [a,b,*], Ivan Fiala [c,d,*]

[a] Department of Aquatic Animal Medicine, College of Fisheries, Huazhong Agricultural University, Wuhan 430070, China
[b] Hubei Engineering Technology Research Center for Aquatic Animal Diseases Control and Prevention, Wuhan 430070, China
[c] Institute of Parasitology, Biology Centre, Academy of Sciences of the Czech Republic, Branišovská 31, 370 05 České Budějovice, Czech Republic
[d] Faculty of Science, University of South Bohemia, Branišovská 31, 370 05 České Budějovice, Czech Republic

ARTICLE INFO

Article history:
Received 15 November 2018
Received in revised form 28 January 2019
Accepted 3 February 2019
Available online 9 May 2019

Keywords:
Myxobolus
Henneguya
Character evolution
Ultrastructure
Phylogenetic analysis

ABSTRACT

Genera *Myxobolus* Bütschli, 1882 and *Henneguya* Thélohan, 1892 (Myxobolidae) are specious myxozoan genera. They comprise nearly half of overall known myxozoan species diversity. A typical spore feature of *Henneguya* is the presence of two caudal appendages of the spore valves, which distinguishes them from species of the genus *Myxobolus*. Several *Myxobolus* spp., however, were reported to show aberrant spores with *Henneguya*-like caudal appendages. We found such aberrant spores in *Myxobolus tsangwuensis* and *Myxobolus wulii*. We studied the ultrastructure of *M. wulii* and *Myxobolus oralis* spores with caudal appendages by transmission electron microscopy (TEM). TEM of these aberrant spores revealed that their caudal appendages have the same ultrastructure as the appendages of *Henneguya* spp. Small caudal appendages of *M. wulii* spores observed only on TEM suggested that this character may be often overlooked and more *Myxobolus* species potentially have the ability to express the caudal appendages on the myxospore. In order to trace the evolution of this character, we performed broad phylogenetic analysis of all species of the family Myxobolidae which are available in GenBank including nearly 300 taxa. We found at least eight independent evolutionary origins of spores with two appendages, three origins of a single appendage and 12 apparent secondary losses of the spore projections. Therefore, genus *Henneguya* with typical two-tailed myxospores is polyphyletic, however a majority of its species has a common ancestor and groups in the second largest subclade of the *Myxobolus* clade. We also mapped the biological characteristics (host, site of infection and environment) of Myxobolidae species on the phylogenetic tree. We revealed an evident host-associated evolutionary pattern in all parts of the *Myxobolus* clade with a distinct and species-rich subclade containing almost exclusively species infecting species of the Order Cypriniformes.

1. Introduction

Myxosporeans are a morphologically and biologically diverse group of cnidarian endoparasites with approximately 2600 species described (Okamura et al., 2018). Most of them infect aquatic animals, especially fish, and less frequently other poikilothermic and homoeothermic vertebrates such as amphibians, reptiles, birds and mammals (Friedrich et al., 2000; Eiras, 2005; Prunescu et al., 2007; Bartholomew et al., 2008). Myxosporean life cycles require an invertebrate definitive host (typically oligochaete or polychaete) that releases actinospore stages, which are infective to the vertebrate intermediate host, to complete the life cycle (Wolf and Markiw, 1984).

Myxosporean taxonomy is mostly based on myxospore morphology, mainly the number and configuration of shell valves and polar capsules (Shulman, 1966; Lom and Noble, 1984). Classification also takes into account many additional details of the myxospore structure as described by Lom and Arthur (1989), such as the presence of caudal projections, the presence of ribs, ridges and striations on the spore valves, the number of turns of polar filament, the mutual size relation of polar capsules or the presence of a mucous envelope, the number of sporoplasms etc. Most of these morphological details are important for differentiation of myxosporeans at the species level. One of the exceptions is the presence/absence and the nature of myxospore caudal projections

* Corresponding authors at: Department of Aquatic Animal Medicine, College of Fisheries, Huazhong Agricultural University, Wuhan 430070, China. Fax: +86 27 87282114 (Zemao Gu). Institute of Parasitology, Biology Centre, Academy of Sciences of the Czech Republic, Branišovská 31, 370 05 České Budějovice, Czech Republic. Fax: +420 385310388 (I. Fiala).
E-mail addresses: guzemao@mail.hzau.edu.cn (Z. Gu), fiala@paru.cas.cz (I. Fiala).

https://doi.org/10.1016/j.ijpara.2019.02.009
0020-7519/

which are the main distinguishing character of the genus *Myxobolus*, *Henneguya*, *Hennegoides* and *Unicauda* (Lom and Dyková, 2006).

Myxobolus Bütschli, 1882 and *Henneguya* Thélohan, 1892 are the most species rich genera within the Myxozoa. Almost half of the myxozoan diversity is concentrated into these two genera with more than 850 *Myxobolus* spp. (Eiras et al., 2014) and 200 species of the genus *Henneguya* (Eiras and Adriano, 2012) described. Taxonomically, they are classified to the family Myxobolidae including another 12 genera with similar spore morphology and the preference of infecting tissues rather than body cavities of freshwater fishes. They can produce large polysporic plasmodia in the tissues and may cause severe diseases (Lom and Dyková, 2006). Fourteen genera of Myxobolidae differ by the number of polar capsule(s) and the presence and number of spore projection(s) (Lom and Dyková, 2006; Sarkar, 2009). *Myxobolus* spp. are characterized by the ellipsoidal or rounded spores with two polar capsules lying in the sutural plane. Spores of *Henneguya* spp. are similar to those of *Myxobolus,* differing only in the presence of two caudal appendages. These structures represent valve extensions at the posterior part of the spore. The *Myxobolus* spore morphotype is simple and can be considered a primary morphotype within Myxobolidae from which other spore morphotypes such as *Henneguya* (two caudal appendages), *Unicauda* (one caudal appendage) or *Thelohanellus* (reduced polar capsule) evolved (Fiala and Bartošová, 2010).

Molecular taxonomy based on the ssrRNA gene does not support the classical spore-based taxonomic classification of Myxobolidae (e.g. Kent et al., 2001; Fiala, 2006; Fiala and Bartošová, 2010). In phylogenetic trees, the positions of many species often disagree with the expected relationships deduced from the taxonomy based on the spore morphology. Kent et al. (2001) already speculated, in their first broad phylogenetic analysis of the Myxosporea, that the caudal appendages of *Henneguya* spp. were not a valid feature for a characterization of the genus. Increasing numbers of available sequence data supported the paraphyletic character of the genus *Myxobolus* with a number of *Henneguya* spp. clustering within the *Myxobolus* clade (e.g. Fiala, 2006; Liu et al., 2010). Eszterbauer (2004) found that the preference for a particular site of development rather than spore morphology is an important criterion for the phylogenetic relationships within *Myxobolus* spp. Later Carriero et al. (2013) demonstrated relationships among *Myxobolus* and *Henneguya* spp. clustering in correlation with the fish taxonomic classification (order or family level). The validity of caudal projections as a taxonomic character was not only called into doubt by phylogenetic analyses but also by the discoveries that a percentage of *Myxobolus* spp. develop within single plasmodium spores with the *Henneguya*-like caudal appendages e.g. *Myxobolus heterosporus*, *Myxobolus bizerti*, *Myxobolus muelleri*, *Myxobolus turpisrotundus*, *Myxobolus musseliusae* and *Myxobolus oralis* (Bahri, 2008; El-Mansy, 2005; Liu et al., 2010, Liu et al., 2013, Liu et al., 2014).

In our work we aimed to i) perform a broad phylogenetic analysis including all species with ssrDNA available in GenBank in order to infer current relationships within Myxobolidae, ii) to map trait evolution of the spore caudal appendages within Myxobolidae, iii) to investigate the development of the caudal appendages on spores of *Myxobolus* and *Henneguya* spp. during spore formation and iv) to evaluate biological aspects (e.g. host preference) that shape the evolution of Myxobolidae.

2. Materials and methods

2.1. Collection of myxospores

Fresh spores of nine *Myxobolus* spp. and *Henneguya doneci* were collected from their hosts in Hubei Province in China during 2009–2013 (Table 1). Samples were checked carefully by microscopic observation to ensure that they contained spores of only one species. Light microscopy was performed on an Olympus BX53 microscope (Olympus optical Co. Ltd., Japan) equipped with an Olympus DP73 camera (Olympus optical Co. Ltd., Japan).

2.2. Ultrastructural examination

Isolated spores of *M. oralis*, *Myxobolus wulii* and *Henneguya doneci* were fixed in 3% glutaraldehyde (Sigma-Aldrich, St. Louis, USA) in 0.2 M sodium cacodylate (SINOPHARM, Shanghai, China) buffer (pH 7.2) at 4 °C overnight and post-fixed in 2% OsO_4 (Greenlight, Beijing, China) buffered with the same solution for 4 h at the same temperature. Following an ethanol series and propylene oxide dehydration, samples were embedded in Epon812 (Emicron, Shanghai, China). Semithin sections were stained with Toluidine blue (Sigma-Aldrich, St. Louis, USA). Ultrathin sections, double contrasted with uranyl acetate and lead citrate, were observed using a HITACHI H-7650 transmission electron microscope (Hitachi, Tokyo, Japan) at 75 kV.

2.3. DNA isolation, PCR and sequencing

Genomic DNA was extracted from fresh spores or the samples fixed in 100% ethanol using a BioTeke™ Genomic DNA extraction kit (BioTeke Co., Ltd, Beijing) according to the manufacturer's protocol. The ssrRNA gene was PCR amplified with a set of universal eukaryotic primers (18e, 5-CTGGTTGATTCTGCCAGT-3 (Hillis and Dixon, 1991) and 18R, 5-CTACGGAAACCTTGTTACG-3 (Whipps et al., 2003)) to obtain an almost complete sequence. PCR was carried out in a 50 μl reaction volume containing approximate 200 ng of extracted genomic DNA, 1×*Taq* Buffer (MBI Fermentas, Vilnius, Lithuania), 2.5 mM $MgCl_2$, 0.2 mM dNTPs (MBI Fermentas), 2 μM each primer, and 2.5 U of *Taq* DNA polymerase (MBI Fermentas) in MilliQ purified water. An EDC-810 DNA Engine (EastWin Bio., Co., Ltd, Beijing) was used to control the cycling conditions: 95 °C for 50 s, 48 °C for 50 s, and 72 °C for 120 s for 35 cycles, with an initial denaturation at 95 °C for 5 min, and a terminal extension at 72 °C for 7 min. In the case of negative or non-specific results, 1 μl of the initial PCR with 18e/18R primers was used as a template for nested PCR with the myxozoan-specific ssrRNA gene primers (see Table 1). The PCR conditions were the same as for the first PCR, with an annealing temperature of 54 °C instead of 48 °C. The PCR products were purified using the AxyPrep™ DNA Gel Extraction Kit (AxyGen Bio., Co., Ltd, Hangzhou, China) and sequenced directly in both directions using the ABI PRISM® 3730XL DNA sequencer (Applied Biosystems Inc., Foster City, CA, USA).

2.4. Phylogenetic analysis

The overlapping partial sequences of ssrDNA were assembled into the contigs in the SeqMan II program v5.05 (DNASTAR Inc., Madison, Wisconsin, USA). An alignment based on ssrDNA sequences was created in the program MAFFT v6.864 (Katoh et al., 2002) using the E-INS-i strategy with default parameters including newly sequenced myxosporeans and all sequences available in GenBank for the family Myxobolidae (297 taxa). Two myxosporean species from the freshwater lineage were selected as an outgroup. Highly variable parts of the alignment were determined and manually excluded in SeaView v4 (Gouy et al., 2010).

Phylogenetic analyses were performed using maximum likelihood (ML) and Bayesian inference (BI). ML was done in RAxML v8.2.11 (Stamatakis, 2006) with a GTR GAMMA model of evolution selected by jModelTest2 (Posada, 2008). Bootstrap supports were calculated from 1000 replicates. BI was computed in MrBayes v3.2.6 (Ronquist and Huelsenbeck, 2003) with the GTR + Γ model

Table 1
List of Myxobolidae spp. used in the phylogenetic reconstruction with information about their site of infection, host fish species, fish order geography, biogeography realm, environment and their ssrDNA sequence GenBank accession number and appropriate reference.

Myxosporean species	Host	Site of infection	ssrDNA		
			GenBank Acc. No.	Sequence length (bp)	Primer pairs
Henneguya doneci	*Carassius auratus gibelio*	Gills	KJ725083	1609	SphF-SphR, MyxospecF-MyxospecR
Myxobolus allotypica	*Hypophthalmichthys molitrix*	Gill rakers	KJ725075	1520	MX5-MX3
Myxobolus honghuensis	*C. auratus gibelio*	Pharynx	KJ725074	1928	18e-18R
Myxobolus koi	*Cyprinus carpio*	Gills	KJ725077	1646	MkoiF-MkoiR
Myxobolus musseliusae[a]	*C. carpio*	Gills	MK141708	1566	SphF-SphR
Myxobolus nielii	*C. auratus gibelio*	Gills	KJ725084	1360	SphF-SphR, MyxospecF-MyxospecR
Myxobolus oralis[a]	*C. auratus gibelio*	Palate of the mouth	KC315782	1615	SphF-SphR, MyxospecF-MyxospecR
Myxobolus.tsangwuensis[a]	*C. carpio*	Gills	KJ725076	1342	SphF-SphR
Myxobolus turpisrotundus[a]	*C. auratus gibelio*	Skin, jaws, gills, fins	KJ725073	1573	MX5-MX3
Myxobolus wulii[a]	*C. auratus gibelio*	Gills, liver	KJ725081	1528	MX5-MX3

References for primers used in the study: SphF and SphR in Eszterbauer and Székely (2004), 18e in Hillis and Dixon (1991), 18R in Whipps et al. (2003), MX5 and MX3 in Andree et al. (1998), MyxospecF and MyxospecR in Fiala (2006), MkoiF (5′-CAGTTTATTGGCGTAGTCG-3′) and MkoiR (5′-TACAATGTCCAGTCCCAGAG -3′) designed in the present study. The spores of *M. turpisrotundus* and *M. wulii* were collected from the host fins and liver, respectively.
[a] *Myxobolus* species with aberrant spores present.

of evolution. Posterior probabilities were calculated over 5,000,000 generations via two independent runs of four simultaneous Markov chain Monte Carlo chains with every 100th tree saved. Tracer v1.4.1 (Rambaut et al., 2018) was used to set the length of the burn-in period.

2.5. Tracing the character evolution of caudal appendages

The ML ssrDNA-based tree generated as described in Section 2.4 was chosen for the reconstruction of ancestral states for the morphological character of caudal appendages. We simulated myxosporean character evolution using the Mesquite program 3.31 (Maddison, W. P., Maddison, D.R., 2017. Mesquite: a modular system for evolutionary analysis. Version 3.31 http://mesquiteproject.org) for the reconstruction of character states at ancestral nodes by the likelihood method using a Markov k-state 1 parameter model with the single parameter. Three character states were set: 0 = none, 1 = one and 2 = two caudal appendages.

3. Results

3.1. Morphology of aberrant Myxobolus spores with spore appendages

Five out of nine *Myxobolus* spp. under study showed the aberrant spore morphology in prolongation of the spore valves. We confirmed the occurrence of aberrant spores in *M. turpisrotundus*, *M. musseliusae*, and *M. oralis* (Liu et al., 2010, Liu et al., 2013, Liu et al., 2014). Here, we newly report the aberrant spores of *M. tsangwuensis* and *M. wulii* (Figs. 1 and 2A). The proportion of aberrant spores with regard to normal ones without appendages was 2% in *M. tsangwuensis* ($n = 500$) and 5% in *M. wulii* ($n = 20$, based on transmission electron microscope (TEM). The length of the caudal projections of *M. tsangwuensis* observed by light microscope ranges from 3.0 to 14.9 μm. Short appendages on aberrant spores of *M. wulii* were observed only by TEM, therefore the exact length of the projections could not be determined.

Ultrastructure of *M. oralis* (Fig. 2B,C) showed that two valves, composed of an outer translucent layer and a central dense core, surrounded the spore and joined together at the sutural ridge. The caudal appendages of the aberrant spore originated posteriolaterally or posteriofrontally from the sutural ridge at the posterior end of the spore. The density of caudal appendage is identical to that of its valve. The structure of the valve of *H. doneci* (Fig. 2D–H) is similar to that of *M. oralis*. In the early developmental phase of the caudal appendage origin, each valve of *H. doneci* elongated posteriofrontally to form a short tail in the posterior region of the spore (Fig. 2D,E). Then, the caudal appendages matured and reached their final dimensions (Fig. 2F–H). The composition of the caudal appendage is identical to that of its valve (Fig. 1E,G, H). TEM revealed a short tail that originated from the extension on the valve of the spore of *M. wulii* (Fig. 2A). However, no aberrant spores were observed under a light microscope.

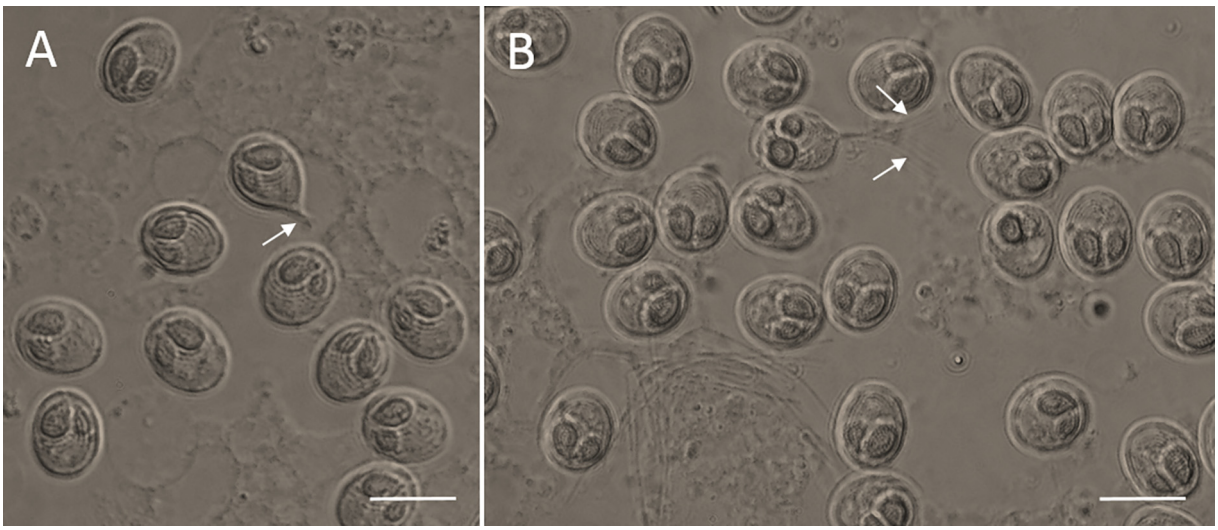

Fig. 1. Aberrant spores of *Myxobolus tsangwuensis* with caudal appendages. (A) Short caudal appendages (arrow) and (B) long caudal appendages (arrow). Scale bar = 10 μm.

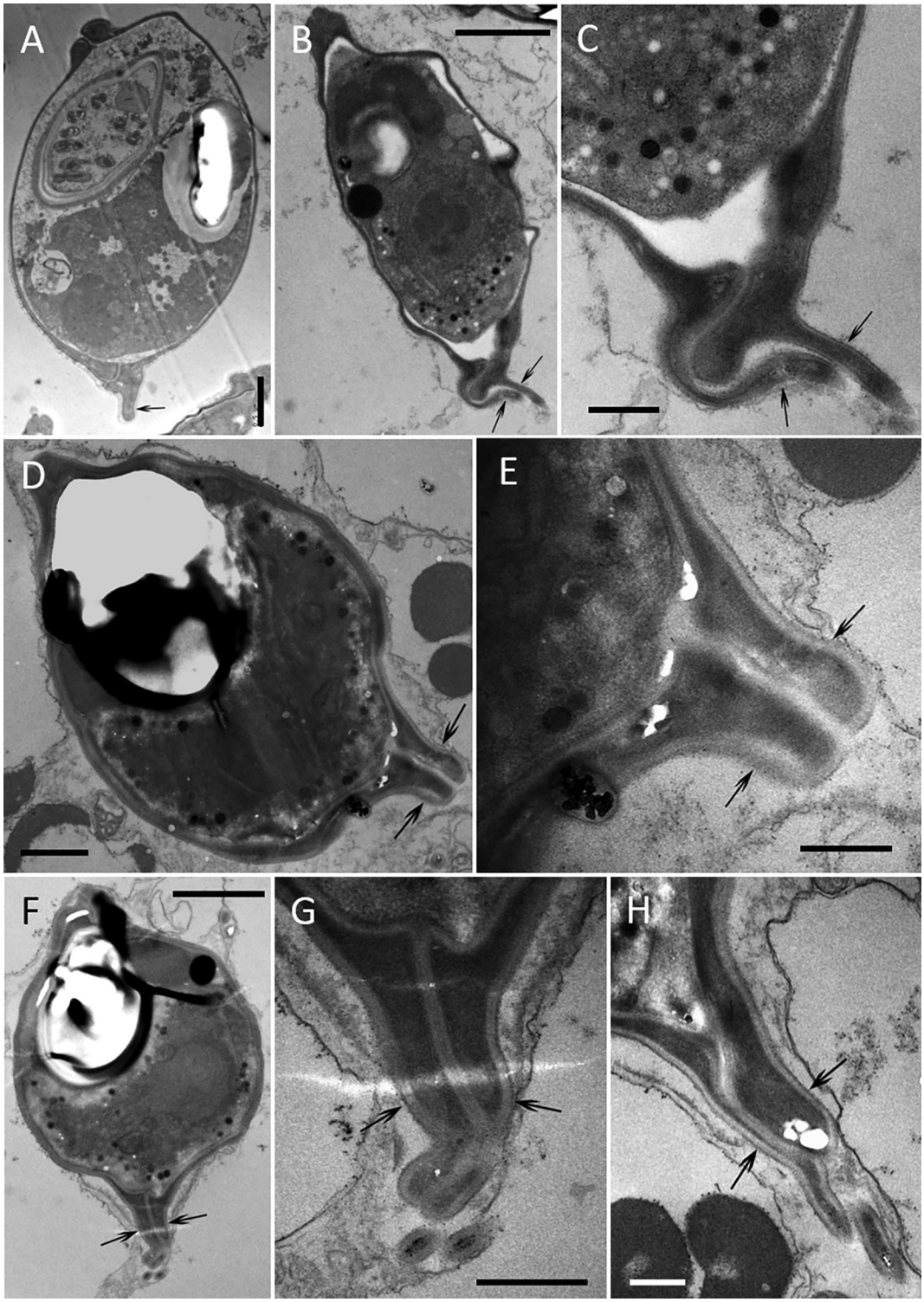

Fig. 2. Ultrastructure of *Myxobolus* and *Henneguya* spp. (A) A short tail (arrow) originated from the extension on the valve of the spore of *Myxobolus wulii*; scale bar = 0.5 μm. (B) The caudal appendages (arrows) originated from the extension on the valve of the spore of *Myxobolus oralis*; scale bar = 2 μm. (C) The magnification of the caudal appendages (arrows) in B; scale bar = 0.5 μm. (D) A short tail (arrows) originated from the extension on the valve of the spore of *Henneguya doneci*; scale bar = 1 μm. (E) The magnification of the short tail (arrows) in D; black arrow head = translucent layer, asterisk = central dense core, scale bar = 0.5 μm. (F) The more obvious caudal appendages (arrows) of *H. doneci*; scale bar = 2 μm. (G) The magnification of the obvious caudal appendages (arrows) in F; white arrow head = sutural ridge, scale bar = 0.5 μm. (H) The developed caudal appendages (arrows) of *H. doneci*; scale bar = 0.5 μm.

3.2. Phylogenetic analyses

We obtained partial ssrDNA sequences of nine *Myxobolus* spp. including five with aberrant spores (Table 1). Their sequences were identical with their counterparts available in GenBank or differ by a maximam of four nucleotides (99.74% identity) in the case of *M. wulii*. ssrDNA of *Myxobolus allotypica* was sequenced, to our knowledge, for the first time. The phylogenetic analysis revealed that *M. allotypica* is very closely related to *M. pavlovskii* (Fig. 3, 96.91% identity), a myxosporean species infecting the same fish host.

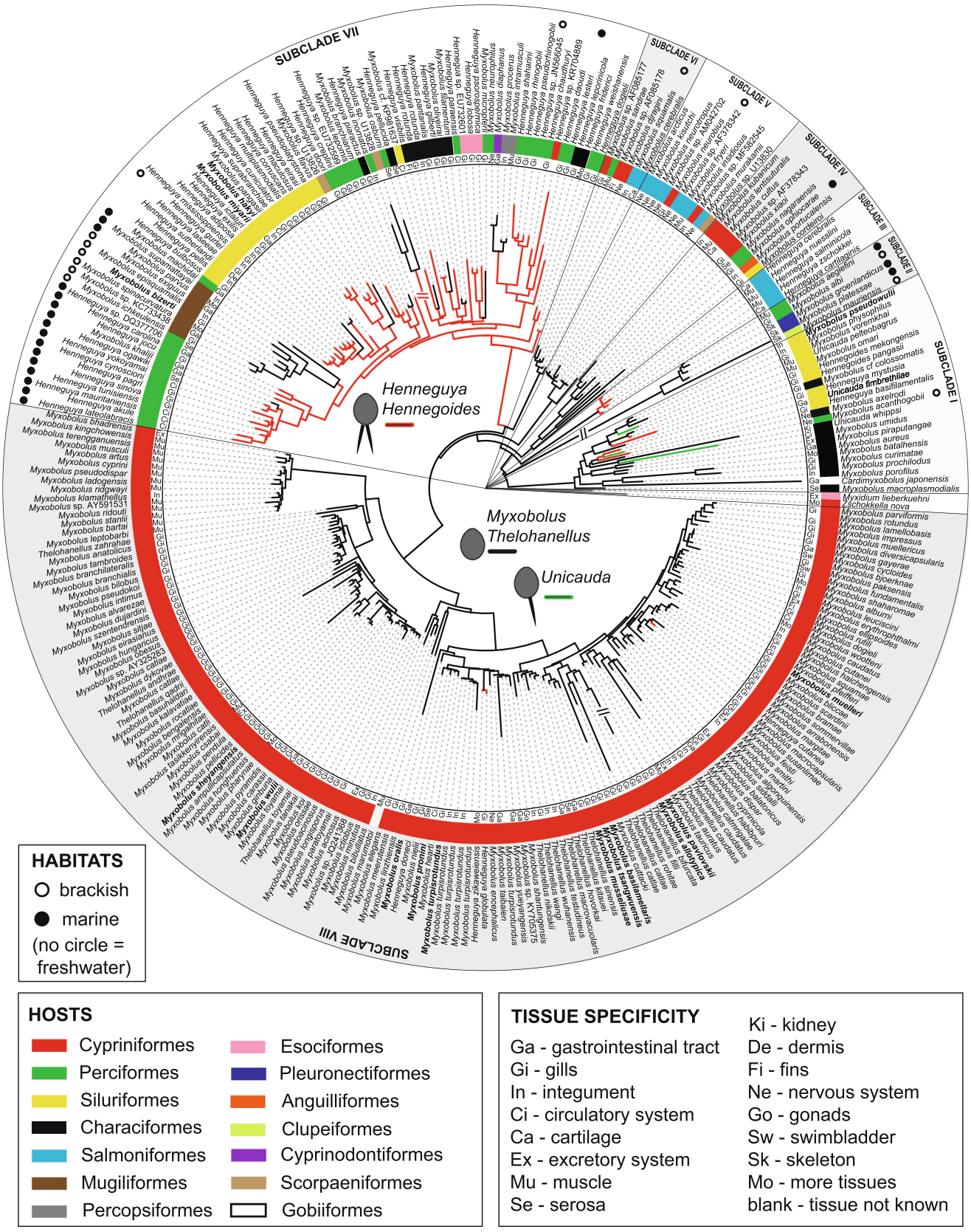

Fig. 3. Phylogenetic reconstruction of the *Myxobolus* clade inferred by the maximum likelihood method (297 taxa). Myxospore morphotypes (*Myxobolus*, *Henneguya* and *Unicauda*) are marked with different colored branches. As well details of host taxonomic classification, tissue specificity and the habitat of the fish host are provided. Aberrant *Myxobolus* spores with caudal appendages are in bold. Nodal supports are provided in Supplementary Fig. S1 and GenBank accession numbers are listed in Supplementary Table S1.

In order to explore the phylogenetic distribution and evolutionary origin of "tailed" Myxobolidae species within the *Myxobolus* clade, as well as the position of *Myxobolus* spp. with aberrant spores, we analysed all currently available 297 ssrDNA sequences of myxosporean species belonging to the *Myxobolus* clade (species of six myxosporean genera *Cardimyxobolus, Hennegoides, Henneguya, Myxobolus, Thelohanellus,* and *Unicauda*). A ssrDNA sequence of *M. spirosulcatus* was not added to the analysis because although it has the *Myxobolus* morphology, this species clustered outside the *Myxobolus* clade in a close relationship with the freshwater *Zschokkella* spp. The species rich *Myxobolus* clade splits into eight distinct subclades (labelled as I – VIII; Fig. 3) that were defined by high nodal support, branch length and stability in the performed phylogenetic analysis (Supplementary Fig. S1). Species in large subclades VII and VIII could be divided by these criteria into more subclades but we kept them in these two because we took into account that subclade VII includes species with a clear *Henneguya* ancestor and subclade VIII is a group of almost exclusively cyprinid infecting species. The relationships among these subclades are generally weakly supported (low nodal supports), therefore the branching pattern of the main subclades differs in the phylogenetic analyses performed. A ML analysis fully resolved all the nodes as shown in Fig. 3, whereas a BI and ML consensus bootstrap tree suggested unresolved polytomy at many nodes (Supplementary Fig. S1).

Myxobolus spp. are present in all eight subclades. Subclade I is a remarkable group of 23 species that are classified into five out of six genera clustering in the *Myxobolus* clade. Six species are tailed forms belonging into the three genera *Henneguya*, *Hennegoides* and *Unicauda*. One of the basal species of this clade is *Cardimyxobolus japonensis* with the unique morphological feature of polar capsules pointing to opposite lateral sides of the spore. Subclades II, IV, V and VI include only *Myxobolus* spp. i.e myxosporeans with two polar capsules that have not evolved any tail form of myxospore. These *Myxobolus* subclades are relatively small in numbers of species (up to 11 species). Subclade III includes exclusively *Henneguya* spp. (five species) characterized by two caudal appendages and two polar capsules.

Two remaining subclades (VII and VIII) are species rich. Subclade VII currently contains 82 species classified to two genera, *Henneguya* and *Myxobolus*. The most predominant morphotype in this subclade is *Henneguya* with 47 representatives (80% of all *Henneguya* spp.) including the type species *H. psorospermica* Thélohan, 1892. Subclade VIII is the most derived one within the *Myxobolus* diversification and contains 154 sequences: 130 sequences of *Myxobolus* including the type species *M. muelleri* Bütschli, 1882, all 20 currently available sequences of *Thelohanellus* spp. characterized by a single polar capsule and only four *Henneguya* spp.

We mapped the biological characteristics (Supplementary Table S1), i.e. host, site of infection, and environment, of all Myxobolidae species on a phylogenetic tree (Fig. 3). Subclade VIII almost exclusively contains species infecting Cypriniformes. The only exception is *Myxobolus marumotoi* from Gobiiformes. A similar host-associated phylogenetic pattern can be seen in subclade VII with groups of closely related species infecting mostly Perciformes, Siluriformes, Mugiliformes and Characiformes. Subclades III and V are mostly composed of parasites of Salmoniformes (with two exceptions from Cypriniformes in subclade V), whereas subclade I includes myxozoans from two fish orders, Siluriformes and Characiformes, with two exceptions found in Perciformes and Gobiiformes. Subclades II, IV and VI include low numbers of species with weak host-associated phylogenetic patterns. The most derived 22 species of subclade VII from Perciformes and Mugiliformes are parasites of marine or brackish fishes. A marine environment is also recorded for *Myxobolus* spp. from subclade II. Among 14 different tissues traced here, gills were found to be the most predominantly targeted fish tissue in the *Myxobolus* clade (Fig. 3). In subclade VIII, there are several groups of species exclusively infecting gills as well as one branch with mostly muscle infecting *Myxobolus* spp. Subclade V consists of species with an affinity mostly to the nervous system. The other subclades did not show any strong association with a particular site of infection.

Our phylogenetic analysis includes 15 *Myxobolus* spp. with reports of an occurrence of aberrant spores with caudal appendages (showed in bold in Fig. 3). However, they did not form a single group of closely related species; several of them clustered together: *Myxobolus basilamellaris*, *M. tsangwuensis* and *M. musseliusae*; *M. oralis*, *M. pronini* and *M. turpisrotundus*; *M. pavlovskii* and *M. allotypica*. All of them plus three others (*M. muelleri*, *M. wulii* and *M. sheyangensis*) cluster in the largest subclade VIII containing cyprinid infecting *Myxobolus* spp. The close relationship of two myxobolids (*Myxobolus hakyi* and *M. miyarii*) with aberrant spores was revealed in subclade VII. This subclade with mostly *Henneguya* spp. also includes *M. bizerti* with aberrant spores. *Myxobolus pseudowulii* is the only representative with aberrant spores in the basal subclade I.

3.3. Evolution of caudal appendages

In order to trace the evolution of caudal spore projections, we reconstructed character states at ancestral nodes and mapped them on the phylogenetic tree of the *Myxobolus* clade (Fig. 3 and Supplementary Fig. S2). Our analysis suggested that the common ancestor of all myxosporeans from the *Myxobolus* clade did not bear the spore projections. Based on the currently available sequenced species, we recorded eight independent origins of spores with two appendages, three origins of a single appendage and 12 apparent secondary losses of the spore projections within the *Myxobolus* evolution. Two independent origins of spore appendages are represented by the common ancestors of subclades III and VII (Supplementary Fig. S2). The remaining six independent origins of this character are represented by extant species without appendage ancestry (e.g. *Henneguya doneci* or *Hennegoides pangasii*) or with a very short evolutionary history (common ancestor of *Henneguya globulata* and *H. zikaweiensis*). Most of the secondary losses of caudal appendages happened in the large subclade VII with predominant *Henneguya* spp.

4. Discussion

We analyzed, to our knowledge for the first time, a representative number of sequences of the Myxobolidae to infer their phylogenies and to trace their evolutionary trajectories with a focus on the evolution of tail-like structures of myxospores in the *Myxobolus* clade. We also showed that the ultrastructure of these spore appendages is identical in aberrant *Myxobolus* myxospores and myxospores of the genus *Henneguya*.

The analysis of nearly 300 sequenced species of the family Myxobolidae available in GenBank revealed that *Henneguya* myxospore appendages evolved at least eight times. Based on our analysis, tailed-type spores are not ancestral morphotypes of the *Myxobolus* clade, however caudal projections already appeared several times independently in the first branching subclade I as *Henneguya*, *Hennegoides* and *Unicauda* spore types (Fig. 3). This may suggest that tailed forms evolved early in evolution of the *Myxobolus* clade. However, low bootstrap supports at basal nodes (see Supplementary Fig. S1) and the presence of several long branches in subclade I indicate that this subclade may branch deeper in the myxobolid evolution. The predominant distribution of *Henneguya* spp. is in subclade VII. The ancestor of this subclade was likely species with an *Henneguya* morphotype and during

evolution many species in this subclade lost the appendages to show the *Myxobolus* morphotype. These reverse evolutionary events happened exclusively in subclade VII.

Spore appendages are very likely functional structures that evolved on the myxospore surface to enable better dispersal in the environment (Fiala et al., 2015). Thus the eight independent origins of this trait may be explained by some evolutionary forces that favored tailed spores. The secondary loss of the appendages happened at least 12 times and they may be connected with the fact that energy invested in the appendage formation was not compensated for with major improvements regarding spore dispersal. This commensurate may be related to the fact that the large group of *Myxobolus* spp. clustering in the "*Henneguya*" subclade VII (with the *Henneguya* morphotype evolutionary history) includes mainly parasites of marine fish. In the marine environment, myxospores do not need floating structures for their dispersal due to higher water density and therefore the ancestor of this group may have lost the spore appendages. On the other hand, our analysis suggested that typical freshwater fish of the order Cypriniformes are almost exclusively hosts for Myxobolidae species without appendages (*Myxobolus* and *Thelohanellus*). Only five out of 165 Myxobolidae species infecting cyprinid fish have spore appendages. Siluriformes and Perciformes are preferential hosts for *Henneguya* spp. with two appendages. Therefore, it may be also the character of host tissues that influences the development of caudal appendages. Eiras et al. (2017) reported the influence of host tissue (e.g. shape of gill filaments) on the *Henneguya* cyst shape which consequently affects the distribution and very likely also the shape of myxosporean spores in the plasmodia.

Plasticity in the presence or absence of myxospore caudal appendages may lie in the ability of the parasite to respond to changes that occur during evolution in the host-parasite relationship. Parasites often switch their hosts and subsequently speciate. Subclade VII, where the plasticity of caudal appendage trait, is very frequent, contains *Myxobolus* and *Henneguya* spp. from nine different fish orders. A skip to a very different fish host may be the reason for morphological adaptations of myxospore (loss or appearance of caudal appendages in the case of *Myxobolus*/*Henneguya* spp.) to newly acquired conditions (e. g. host tissue, different environment of fish host).

Although the only morphological difference between the genera *Myxobolus* and *Henneguya* is the presence of two caudal projections on the spore valves of the latter, several *Myxobolus* spp. have the capacity to develop spore projections (e.g. El-Mansy, 2005; Bahri, 2008; Liu et al., 2010, 2013, 2014). The percentage of aberrant *Myxobolus* spores observed in our study in *M. tsangwuensis* and *M. wulii* fit into the percentage range reported for other *Myxobolus* spp. by the above-mentioned authors. The *Myxobolus* spore projections are usually short (less than half of the spore length) compared with the length of most of *Henneguya* spp., however we observed spores of *M. tsangwuensis* with longer projections (Fig. 1B) than the length of the spore which is typical for most *Henneguya* spp.

Since there is no knowledge about the molecular background of formation of spore valves, we can only speculate what the genetic conditions were that caused the appendage formation on spores of *Henneguya*, *Hennegoides*, *Unicauda* and on some aberrant *Myxobolus* spores. The latter may be explained by some malfunction of spore formation during its development. We showed that the posterior part of the spore valve extends into the caudal appendage in the same way as is seen during *Henneguya* spore formation (Fig. 2). We could speculate that having aberrant spores is not an ontogenetic failure but a genetically encoded trait resulting in a percentage of the myxospores with appendages in order to disperse a portion of the myxospores over longer distances. Myxozoans with this ability can spread their spores to a wider area and infect more definitive hosts. This may be a myxozoan evolutionary novelty and a better strategy than having either tailed or tailless forms of myxospores. Recently, three cases of *Myxobolus* spp. were found to develop spores both with and without *Henneguya*-like caudal appendages within a single plasmodium (Liu et al., 2010, Liu et al., 2013, 2014). Compared with the total number of *Myxobolus* spp., the number of reported *Myxobolus* spp. with *Henneguya*-like tails is relatively low, however caudal appendages may be easily overlooked. We experienced this in *M. wulii* spores which under light microscopy did not show any spore appendages, but TEM revealed short spore extensions. Thus relatively short caudal appendages on *Myxobolus* spores may not be recorded. Furthermore, species descriptions are usually based on those myxospores only, the shapes of which represent the majority of examined myxospores in the plasmodia and/or in the host. In most cases, aberrant spores are probably not documented, or not even mentioned in a description. Therefore, it is likely that many *Myxobolus* spp. produce myxospores with some percentage of aberrant ones with caudal appendages.

Our analysis strongly supported the host-associated phylogenetic patterns in the *Myxobolus* clade (Carriero et al., 2013; Holzer et al., 2018). Great diversification and species richness of the genus *Myxobolus* is mainly due to host-parasite co-speciation of *Myxobolus* spp. infecting Cypriniform fishes in subclade VIII, in which more than half of all sequenced *Myxobolus* spp. clustered. Interestingly, other subclades contained only a few species infecting Cypriniformes, mainly in subclade IV. Host association was evident in all parts of the *Myxobolus* clade. There were many groups of species infecting the same fish order, e.g. Siluriformes in subclade I and VII, Salmoniformes in subclade III and V, Mugiliformes in subclade VII or large group of marine species infecting perciform fish in subclade VII. Although it seems that the site of infection does not play an important role in the *Myxobolus* clade phylogeny, in the largest subclade VIII containing more than half of the sequenced species, there is a tendency of gill and muscle-infecting species to cluster according to the site of infection as was already observed by Eszterbauer (2004).

Myxobolus and *Henneguya* spp. are typical parasites of freshwater fish, however several independent skips to the marine environment are recorded. The largest species diversity of closely related marine *Myxobolus* and *Henneguya* spp. was in subclade VII as well as all five species in subclade II being from marine or brackish fishes.

Discrepancies between the classical spore-based classification and DNA sequence-based phylogenies have led to a discussion about the validity of the genus *Henneguya* (Kent et al., 2001; Fiala, 2006; Fiala and Bartošová, 2010; Liu et al., 2010; Carriero et al., 2013). Kent et al. (2001) were the first who stressed that the caudal appendages did not represent a valid character for distinction of the genera *Myxobolus* and *Henneguya* based on the first large ssrDNA phylogenetic reconstruction. Although we have strong arguments to suppress the genus *Henneguya* and rename all *Henneguya* spp. as *Myxobolus*, we have not taken this step. The main reason is that the *Myxobolus* clade contains not only *Henneguya* spp., but also species of the genera *Thelohanellus*, *Unicauda*, *Hennegoides* and *Cardimyxobolus*. The branching patterns of these species would not result in monophyly of *Myxobolus*, even if *Henneguya* was suppressed and therefore this large taxonomic change, suppression of one of the most traditional myxozoan genera, would not resolve the issue for taxonomy, which should reflect molecular phylogenetic clustering. Another reason is that *Thelohanellus*, *Unicauda*, *Hennegoides* and *Cardimyxobolus* do not have their type species sequenced and their potential inclusion in *Myxobolus* cannot presently be resolved. Moreover, there are more than 20 species of both *Myxobolus* and *Henneguya* with identical species names. Assigning these *Henneguya* spp. to the genus

Myxobolus would lead to the invention of new species names for the *Henneguya* spp. and to possible confusion in the taxonomy. For example common species *Henneguya percae*, *H. salmonis* or *H. cerebralis* would be classified as *Myxobolus* with new species names because *Myxobolus percae*, *M. salmonis* as well as *M. cerebralis* already exist. Therefore we decided to keep, for now, the genus *Henneguya* in the myxozoan taxonomy even though our analyses show that no clear line exists that separates it from the genus *Myxobolus*. Nevertheless, great expansion and availability of sequencing provides a good prospect of obtaining sequences of the type species of all genera of the Myxobolidae which are necessary for proper taxonomical changes.

Acknowledgements

This work was supported by the Nature Science Foundation of China (grant numbers 31572233, 31501848); the China Agriculture Research System (grant number CARS-46); the Research and Demonstration of Key Techniques for High Quality Aquatic Products, China (grant number 2016620000001046); and the Czech Science Foundation (grants #16-20744S, #505/12/G112). The authors thank Mingjun Huang (College of Fisheries, Huazhong Agricultural University, China) for his help with getting the photomicrograph of the aberrant spores of *Myxobolus tsangwuensis*. The authors are grateful to Astrid Holzer for helpful discussions.

Appendix A. Supplementary data

Supplementary data to this article can be found online at https://doi.org/10.1016/j.ijpara.2019.02.009.

References

Andree, K.B., MacConnell, E., Hedrick, R.P., 1998. A nested polymerase chain reaction for the detection of genomic DNA of *Myxobolus cerebralis* in rainbow trout *Oncorhynchus mykiss*. Dis. Aquat. Org. 34, 145–154.

Bahri, S., 2008. Abnormal forms of *Myxobolus bizerti* and *Myxobolus mülleri* (Myxosporea: Bivalvulida) spores with caudal appendages. Bull. Eur. Assoc. Fish Pathol. 28, 252–255.

Bartholomew, J.L., Atkinson, S.D., Hallett, S.L., Lowenstine, L.J., Garner, M.M., Gardiner, C.H., Rideout, B.A., Keel, M.K., Brown, J.D., 2008. Myxozoan parasitism in waterfowl. Int. J. Parasitol. 38, 1199–1207.

Carriero, M.M., Adriano, E.A., Silva, M.R.M., Ceccarelli, P.S., Maia, A.A.M., 2013. Molecular Phylogeny of the *Myxobolus* and *Henneguya* Genera with Several New South American Species. PLoS One 8, e73713.

Eiras, J.C., 2005. An overview on the myxosporean parasites in amphibians and reptiles. Acta Parasitol. 50, 267–275.

Eiras, J.C., Cruz, M., Cruz, C., Saraiva, A., Adriano, E.A., Székely, C., Molnár, K., 2017. Observations on non-random distribution of spores of *Henneguya* spp. (Cnidaria: Myxosporea: Myxobolidae) within plasmodia. Folia Parasitol. 64, 019.

Eiras, J.C., Zhang, J.Y., Molnár, K., 2014. Synopsis of the species of *Myxobolus* Bütschli, 1882 (Myxozoa: Myxosporea, Myxobolidae) described between 2005 and 2013. Syst. Parasitol. 88, 11–36.

Eiras, J.C., Adriano, E.A., 2012. A checklist of new species of *Henneguya* Thélohan, 1892 (Myxozoa: Myxosporea, myxobolidae) described between 2002 and 2012. Syst. Parasitol. 83, 95–104.

El-Mansy, A., 2005. Revision of *Myxobolus heterosporus* Baker, 1963 (syn. *Myxosoma heterospora*) (Myxozoa: Myxosporea) in African records. Dis. Aquat. Organ. 63, 205–214.

Eszterbauer, E., 2004. Genetic relationship among gill-infecting *Myxobolus* species (Myxosporea) of cyprinids: molecular evidence of importance of tissues pecificity. Dis Aquat. Organ. 58, 35–40.

Eszterbauer, E., Székely, C., 2004. Molecular phylogeny of the kidney-parasitic *Sphaerospora renicola* from common carp (*Cyprinus carpio*) and *Sphaerospora* sp. from goldfish (*Carassius auratus auratus*). Acta Vet. Hung. 52, 469–478.

Fiala, I., 2006. The phylogeny of Myxosporea (Myxozoa) based on small subunit ribosomal RNA gene analysis. Int. J. Parasitol. 36, 1521–1534.

Fiala, I., Bartosova, P., 2010. History of myxozoan character evolution on the basis of rDNA and EF-2 data. BMC Evol. Biol. 10, 288.

Fiala, I., Bartošová-Sojková, P., Okamura, B., Hartikainen, H., 2015. Adaptive radiation and evolution within the myxozoa. In: Okamura, B., Gruhl, A., Bartholomew, J.L. (Eds.), Myxozoan Evolution. Springer International Publishing Switzerland, Ecology and Development, pp. 69–84.

Friedrich, C., Ingolic, E., Freitag, B., Kastberger, G., Hohmann, V., Skofitsch, G., Neumeister, U., Kepka, O., 2000. A myxozoan-like parasite causing xenomas in the brain of the mole, *Talpa europaea* L., 1978 (Vertebrata, Mammalia). Parasitology 121, 483–492.

Gouy, M., Guindon, S., Gascuel, O., 2010. SeaView version 4: a multiplatform graphical user interface for sequence alignment and phylogenetic tree building. Mol. Biol. Evol. 27, 221–224.

Holzer, A.S., Bartošová-Sojková, P., Born-Torrijos, A., Lövy, A., Hartigan, A., Fiala, I., 2018. The joint evolution of the Myxozoa and their alternate hosts: A cnidarian recipe for success and vast biodiversity. Mol. Ecol. 27, 1651–1666.

Hillis, D.M., Dixon, M.T., 1991. Ribosomal DNA: molecular evolution and phylogenetic inference. Quart. Rev. Biol. 66, 411–453.

Kent, M.L., Andree, K.B., Bartholomew, J.L., El-Matbouli, M., Desser, S.S., Devlin, R.H., Feist, S.W., Hedrick, R.P., Hoffmann, R.W., Khattra, J., Hallett, S.L., Lester, R.J.G., Longshaw, M., Palenzeula, O., Siddall, M.E., Xiao, C., 2001. Recent advances in our knowledge of the Myxozoa. J. Eukaryot. Microbiol. 48, 395–413.

Katoh, K., Misawa, K., Kuma, K.I., Miyata, T., 2002. MAFFT: A novel method for rapid multiple sequence alignment based on fast Fourier transform. Nucleic Acids Res. 30, 3059–3066.

Liu, Y., Whipps, C.M., Gu, Z.M., Zeng, L.B., 2010. *Myxobolus turpisrotundus* (Myxosporea: Bivalvulida) spores with caudal appendages: investigating the validity of the genus *Henneguya* with morphological and molecular evidence. Parasitol. Res. 107, 699–706.

Liu, Y., Whipps, C.M., Gu, Z.M., Huang, M.J., He, C., Yang, H.L., Molnár, K., 2013. *Myxobolus musseliusae* (Myxozoa:Myxobolidae) fromthe gills of common carp *Cyprinus carpio* and revision of *Myxobolus dispar* recorded in China. Parasitol. Res. 112, 289–296.

Liu, Y., Whipps, C.M., Nie, P., Gu, Z.M., 2014. *Myxobolus oralis* sp. n. (Myxosporea: Bivalvulida) infecting the palate in the mouth of gibel carp *Carassius auratus gibelio* (Cypriniformes: Cyprinidae). Folia Parasitol. 61, 505–511.

Lom, J., Arthur, J.R., 1989. A guideline for the preparation of species descriptions in Myxosporea. J. Fish Dis. 12, 151–156.

Lom, J., Noble, E., 1984. Revised classification of the myxosporea Bütschli, 1881. Folia Parasitol. 31, 193–205.

Lom, J., Dyková, I., 2006. Myxozoan genera: definition and notes on taxonomy, life-cycle terminology and pathogenic species. Folia Parasitol. 53, 1–36.

Okamura, B., Hartigan, A., Naldoni, J., 2018. Extensive uncharted biodiversity: the parasite dimension. Integr. Comp. Biol., 1–14

Posada, D., 2008. jModelTest: phylogenetic model averaging. Mol. Biol. Evol. 25, 1253–1256.

Prunescu, C.C., Prunescu, P., Pucek, Z., Lom, J., 2007. The first finding of myxosporean development from plasmodia to spores in terrestrial mammals: *Soricimyxum fegati* gen.et sp. n. (Myxozoa) from *Sorex araneus* (Soricomorpha). Folia Parasitol. 54, 159–164.

Rambaut, A., Drummond, A.J., Xie, D., Baele, G., Suchard, M.A., 2018. Posterior summarisation in Bayesian phylogenetics using Tracer 1.7. Syst. Biol, syy032.

Ronquist, F., Huelsenbeck, J.P., 2003. MrBayes 3: Bayesian phylogenetic inference under mixed models. Bioinformatics 19, 1572–1574.

Sarkar, N.K., 2009. *Thelohanelloid bengalensis* gen. and sp. nov. (Myxosporea: Thelohanellidae) from the gall bladder of marine catfish of the Bay of Bengal, India. Uttar Pradesh J. Zool. 29, 251–254.

Shulman, S.S., 1966. Myxosporidia of the Fauna of the USSR. Nauka, Moscow (in Russian).

Stamatakis, A., 2006. RAxML-VI-HPC: Maximum Likelihood-based phylogenetic analyses with thousands of taxa and mixed models. Bioinformatics 22, 2688–2690.

Wolf, K., Markiw, M.E., 1984. Biology contravenes taxonomy in the Myxozoa: new discoveries show alternation of invertebrate and vertebrate hosts. Science 225, 1449–1452.

Whipps, C.M., Adlard, R.D., Bryant, M.S., Lester, R.J.G., Findlay, V., Kent, M.L., 2003. First report of three *Kudoa* species from eastern Australia: *Kudoa thyrsites* from Mahi mahi (*Coryphaena hippurus*), *Kudoa amamiensis* and *Kudoa minithyrsites* n. sp. from Sweeper (*Pempheris ypsilychnus*). J. Eukaryot. Microbiol. 50, 215–219.